ANTIOXIDANTS & REDOX SIGNALING
Volume 18, Number 16, 2013

DOI: 10.1089/ars.2012.5052

Discoveries

FORUM ORIGINAL RESEARCH COMMUNICATION

Functional Analysis of Arabidopsis Mutants Points to Novel Roles for Glutathione in Coupling H_2O_2 to Activation of Salicylic Acid Accumulation and Signaling

Yi Han,[1] Sejir Chaouch,[1] Amna Mhamdi,[1] Guillaume Queval,[1,*] Bernd Zechmann,[2] and Graham Noctor[1]

Abstract

Aims: Through its interaction with H_2O_2, glutathione is a candidate for transmission of signals in plant responses to pathogens, but identification of signaling roles is complicated by its antioxidant function. Using a genetic approach based on a conditional catalase-deficient Arabidopsis mutant, *cat2*, this study aimed at establishing whether GSH plays an important functional role in the transmission of signals downstream of H_2O_2. ***Results:*** Introducing the *cad2* or allelic mutations in the glutathione synthesis pathway into *cat2* blocked H_2O_2-triggered GSH oxidation and accumulation. While no effects on NADP(H) or ascorbate were observed, and H_2O_2-induced decreases in growth were maintained, blocking GSH modulation antagonized salicylic acid (SA) accumulation and SA-dependent responses. Other novel double and triple mutants were produced and compared with *cat2 cad2* at the levels of phenotype, expression of marker genes, nontargeted metabolite profiling, accumulation of SA, and bacterial resistance. Most of the effects of the *cad2* mutation on H_2O_2-triggered responses were distinct from those produced by mutations for GLUTATHIONE REDUCTASE1 (*GR1*) or NONEXPRESSOR OF PATHOGENESIS-RELATED GENES 1 (*NPR1*), and were linked to compromised induction of ISOCHORISMATE SYNTHASE1 (*ICS1*) and ICS1-dependent SA accumulation. ***Innovation:*** A novel genetic approach was used in which GSH content or antioxidative capacity was independently modified in an H_2O_2 signaling background. Analysis of new double and triple mutants allowed us to infer previously undescribed regulatory roles for GSH. ***Conclusion:*** In parallel to its antioxidant role, GSH acts independently of NPR1 to allow increased intracellular H_2O_2 to activate SA signaling, a key defense response in plants. *Antioxid. Redox Signal.* 18, 2106–2121.

Introduction

As potent signal molecules, reactive oxygen species (ROS) play important roles in transmitting information during responses of both plant and animal cells to the environment. Since the seminal studies that established key roles for ROS in plant-pathogen interactions (1, 14, 28), primary redox-linked events have been considered to be extracellular or plasmalemma located, mediated primarily by NADPH oxidases, peroxidases, or other enzymes (6, 13, 41, 60, 61). However, these initial signals at the cell surface/apoplast lead to later downstream adjustments in intracellular redox state (17, 62, 64) that are notably associated with thiol-dependent activation of the cytosolic protein, NONEXPRESSOR OF PATHOGENESIS-RELATED GENES1 (NPR1). Reduction of

Innovation

Over the last two decades, several studies have implicated glutathione in plant interactions with pathogenic organisms. We used a novel genetic approach in which GSH content or antioxidative capacity was independently modified in an H_2O_2 signaling background. The data show that GSH has a key influence in controlling accumulation of the signal molecule salicylic acid (SA) and its dependent responses downstream of H_2O_2, and that this role is not merely due to its antioxidant properties. Exploitation of mutations in the SA synthesis or signaling pathway allowed us to infer previously undescribed regulatory roles for GSH.

[1]Institut de Biologie des Plantes, UMR CNRS 8618, Université de Paris Sud, Orsay Cedex, France.
[2]Institute of Plant Sciences, University of Graz, Graz, Austria.
*Current affiliation: Centre for Plant Sciences, Faculty of Biology, University of Leeds, Leeds, United Kingdom.

NPR1 is required to link a part of the salicylic acid (SA) signaling pathway to induction of genes such as *PATHOGENESIS-RELATED1* (*PR1*; 38).

One of the key players governing intracellular redox state is the thiol/disulfide compound, glutathione (GSH). Several reports have used single mutants or transformants that are deficient in GSH in studies of pathogenesis responses (2, 3, 16, 24, 34, 42). While some of these have described effects of altered GSH status, it remains unknown where GSH acts in the signaling chain and how it interacts with ROS-dependent events. Interpretation of the role of GSH is complicated by its antioxidant function, which depends on regeneration of the thiol form, GSH, from the disulfide form, glutathione disulfide (GSSG), by glutathione reductase (GR). The predominant concept of GSH function is as a negative regulator that acts to oppose or limit H_2O_2 signals. In terms of thiol-dependent signaling functions in pathogenesis responses, the NPR1 pathway remains, by far, the best studied (19, 26, 33). However, although exogenous GSH can induce *PR1* expression, NPR1 reduction has been reported to be mediated through thioredoxin-dependent systems (59). Adding to these uncertainties are recent studies that have revealed the complexity both of NPR1 redox regulation (29) and of potential functional overlap between cytosolic thiol/-disulfide systems (4, 31, 49).

Enhanced oxidation of GSH, accompanied by increases in the total pool, is a well-documented response in plants subjected to treatments such as ozone, cold, pathogens, or SA (5, 17, 21, 26, 34, 53, 62). Photorespiratory catalase (CAT)-deficient plants are model systems in which such changes are particularly evident (44, 50, 56, 67). The interest of these systems is that they allow the role of H_2O_2 signaling to be studied specifically and controllably, because the endogenous signal can be manipulated easily by external conditions (12, 37). When conditions allow active photorespiration, increased H_2O_2 availability in the Arabidopsis knockout *cat2* mutant triggers accumulation of GSH followed by induction of pathogenesis responses in the absence of pathogen challenge (9, 44). The well-defined changes in GSH in CAT-deficient plants are useful as a readout of altered redox state, but their functional impact is unclear. It remains to be established whether they play any role in coupling H_2O_2 to downstream defense responses or are rather an accompanying, passive response of the cell to enhanced H_2O_2.

Increases in H_2O_2 in CAT-deficient plants are much less apparent and reproducible than those observed in GSH (37), raising the possibility that some of the signals downstream of intracellular H_2O_2 may be mediated by changes in GSH status. Altered GSH status in CAT-deficient plants or in response to stress presumably reflects an increased load on reductant-requiring antioxidant pathways. This is underscored by analysis of Arabidopsis *gr1* knockout mutants for one of the two GR-encoding genes. While glutathione reductase 1 (GR1) deficiency does not in itself lead to an oxidative stress phenotype, the *gr1* mutation greatly enhances stress in the *cat2* background, showing that GSH-dependent antioxidative pathways are increasingly solicited when CAT activity is compromised (36).

By exploiting *cat2* as a model H_2O_2 signaling background, we recently reported evidence that intracellular oxidative stress interacts with specific NADPH oxidases to determine activation of SA accumulation and SA-dependent pathways. The *atrbohF* mutant lacking expression of a specific NADPH oxidase shows compromised SA accumulation and resistance to virulent bacteria, and also attenuates *cat2*-triggered SA accumulation and induced resistance (10). Intriguingly, the clearest indicator of redox interactions between the *cat2* and *atrbohF* mutations was not H_2O_2 itself but the status of GSH: Attenuation of SA contents and SA-dependent responses was correlated with decreased accumulation of GSH in *cat2 atrbohF* compared with *cat2* (10).

In this study, we report a targeted analysis of the role of GSH status in transmitting H_2O_2 responses. We chose the *cat2* mutant as a well-defined conditional redox signaling system in which H_2O_2 provokes oxidative modulation of the GSH pool accompanied by activation of SA signaling and associated pathogenesis-related responses. We sought to elucidate the relationship between enhanced H_2O_2 production, the response of GSH, and the activation of the SA pathway by answering the following specific questions. (1) Does GSH play a specific role in H_2O_2 signaling, independent of other potentially redundant thiol systems? (2) To what extent is any such role dependent on GSH status, rather than GSH redox turnover in an antioxidant function? (3) What is the relationship between GSH status and NPR1 function in transmitting signals downstream of H_2O_2? To examine these questions, we exploited mutant lines available in Arabidopsis that have decreased GSH or SA, or loss of GR1 or NPR1 function (Supplementary Table S1; Supplementary Data are available online at www.liebertpub.com/ars). By functional analysis of the effects of these specific mutations in the *cat2* H_2O_2 signaling background, we infer previously unidentified roles for GSH in controlling oxidative stress-triggered SA signaling.

Results

Plants deficient in the major leaf CAT show accumulation of GSH that is conditional on H_2O_2 production through photorespiration (44). When *cat2* is grown in air in moderate light, GSH accumulation accompanies the appearance of lesions, which initially develop after about two weeks of growth and then spread to cover about 15% total rosette area within the next week. This is associated with induction of SA-dependent *PR* genes and enhanced resistance to bacteria. All these H_2O_2-triggered effects in *cat2*, except GSH accumulation, can be reverted by the *sid2* mutation (9), which blocks SA synthesis through the isochorismate synthase (ICS1)-dependent pathway (66). During growth at high CO_2, where photorespiratory glycolate oxidase activity is negligible, *cat2* shows no signs of oxidative stress and is phenotypically indistinguishable from the wild-type Col-0. However, when plants grown first at high CO_2 are transferred to air, GSH in *cat2* accumulates to similar levels to those observed in *cat2* grown in air from seed. This effect is followed by initiation of pathogenesis-related responses about five days after transfer to air and their continued development during subsequent days (10). These features allow *cat2* to be used as a conditional model in which the roles of GSH in defense signaling triggered by intracellular oxidative stress can be examined either during growth in air from seed or by the induced stress that follows the transfer of plants from high CO_2 to air. As we report in this study, both conditions allow activation of the SA pathway in the *cat2* mutant. However, studying responses after transfer from high CO_2 to air is particularly useful for double mutants in which the interpretation is complicated by their extreme phenotypes when they are grown from seed in

air. Thus, for some experiments, transfer from the high CO_2 condition was preferred as a protocol for inducing oxidative stress. However, the principal effects of GSH on the SA pathway that we report here were observed using both experimental protocols.

Genetic blocks over H_2O_2-triggered GSH accumulation inhibit cell death and associated pathogenesis responses induced by intracellular oxidative stress

When *cat2* plants were grown in nonstress conditions (at high CO_2), leaf GSH remained at wild-type levels and reduction state (about 95% reduced). Within 4 h after transfer to air from high CO_2, the reduction state in *cat2* fell from 95% to 61% reduced (Fig. 1A). GSH oxidation continued in *cat2* on subsequent days, and the pool was more than 50% oxidized 4 days after transfer. This oxidation was accompanied by a more than two-fold increase in the total pool. The *cat2*-triggered oxidation and accumulation of GSH were blocked by the *cad2* mutation: in *cat2 cad2*; GSH remained about 90% reduced, and was only slightly increased above *cad2* levels after 4 days of exposure to air (Fig. 1A). In contrast to the effects of the *cat2* and *cad2* mutations on GSH, two major intracellular redox pools that GSH donates electrons to (ascorbate) or receives electrons from (NADPH) were much less affected. Ascorbate reduction status was above 80% in all lines, while NADP(H) pools were constant between 50% and 60% reduced. Thus, when plants are grown in conditions permissive for photorespiratory H_2O_2 production, the *cat2* mutation triggers a response of the GSH pool that is quite specific, and introduction of the *cad2* mutation produces a specific block on this response.

Studies of plants deficient in CAT grown in different conditions suggest that the GSH pool is in close correspondence to the predicted H_2O_2 availability (37, 44). We have previously reported that H_2O_2 itself (measured as *in situ* staining or extractable H_2O_2) is minor or undetectable in *cat2*, even when plants are clearly undergoing oxidative stress (9, 10, 36). In the present study, we re-examined extractable peroxides in *cat2* and compared levels with those found in *cat2 cad2* at two time points after transfer to oxidative stress conditions. For comparison, we included the *cat2 gr1* double mutant, in which loss of *GR1* function exacerbates oxidative stress compared with *cat2* (36). At 4 days after transfer from high CO_2 to air, no difference was apparent between any of the lines, suggesting that any excess H_2O_2 had been efficiently metabolized at this point (Fig. 1B). At 4 h after transfer, however, a 60% increase in peroxides relative to Col-0 was detected in *cat2*, and this increase was slightly more pronounced in the *cat2 gr1* double mutant (Fig. 1B). In *cat2 cad2* at this early time point, peroxides were intermediate between Col-0 and *cat2*. Together, these findings show that when placed in air, the *cat2* background causes an accumulation of H_2O_2 that is transient and relatively minor, suggesting that other, reductive systems are able to replace the major leaf CAT in efficiently metabolizing photorespiratory H_2O_2 when *CAT2* function is lost. Its marked, progressive perturbation in *cat2* implicates GSH as a significant component in these reductive systems. Thus, the *cat2 cad2* mutant offers an interesting system to establish the functional significance of H_2O_2-triggered adjustments in GSH.

To examine how the *cad2* mutation affects the subcellular distribution of GSH in *cat2* in oxidative stress conditions, we exploited a specific antibody to quantify GSH pools in different compartments (69, 70). In agreement with the increase in total tissue GSH (Fig. 1), immunogold labeling was significantly increased in *cat2* compared with Col-0 (Fig. 2A). This increase was mainly due to enhanced signal in chloroplasts, vacuoles, and the cytosol (Fig. 2B). All these effects

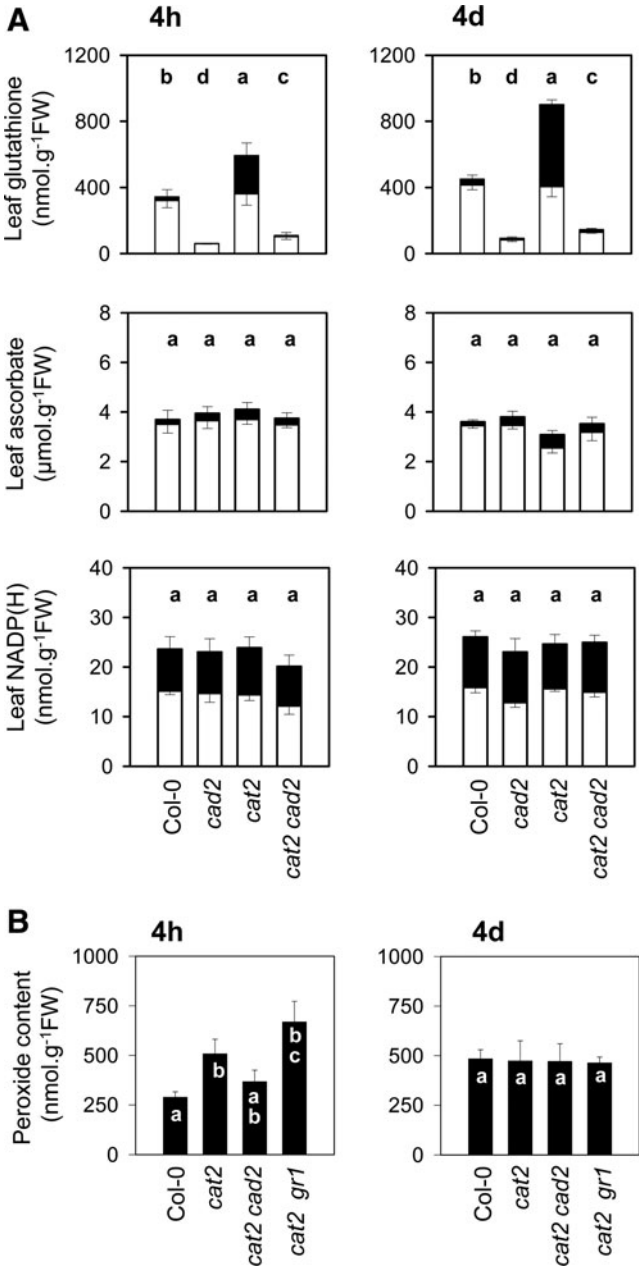

FIG. 1. Oxidant and antioxidant capacity in plant lines with modulated glutathione contents. (A) Leaf contents of NADP(H), ascorbate, and GSH in Col-0, *cad2*, *cat2*, and *cat2 cad2*. White bars, reduced forms. Black bars, oxidized forms. **(B)** Leaf peroxide contents in Col-0, *cat2*, *cat2 cad2*, and *cat2 gr1*. Plants were grown at high CO_2, where the *cat2* mutation is silent, then transferred to air to initiate oxidative stress in the *cat2* backgrounds. Samples were taken 4 h and 4 days after transfer. Data are means ± SE of at least three biological repeats. Different letters indicate significant difference at $p < 0.05$ for leaf contents. Note that *x*-axis legends to parts **A** and **B** are different.

were annulled by the *cad2* mutation. In *cat2 cad2*, GSH was decreased in all measured compartments, especially the chloroplast, cytosol, nucleus, and peroxisomes (Fig. 2). From multiple images of photosynthetic mesophyll cells, subcellular GSH concentrations were estimated in the three lines (see Materials and methods for details). They ranged from 1–10 m*M* in Col-0 and *cat2*, whereas concentrations in all compartments except the mitochondria did not greatly exceed 1 m*M* in *cat2 cad2* (Table 1).

Table 1. Subcellular Glutathione Concentrations in Col-0, *cat2*, and *cat2 cad2*

	Col-0	*cat2*	*cat2 cad2*
Cytosol	4.8	7.4	0.8
Nuclei	7.5	9.0	1.2
Chloroplasts	1.1	2.7	0.1
Mitochondria	10.3	10.1	7.5
Peroxisomes	5.4	6.0	0.8
Vacuole	0.04	0.5	0.03

Plants were grown as described for Figure 1. Values are in m*M* and were calculated from relative gold labeling densities as described in Materials and Methods based on mean values of multiple counts of different cells ($n > 20$ for peroxisomes and vacuoles, and $n > 60$ for all other cell compartments).

The effect of genetically blocking GSH accumulation on H_2O_2-triggered pathogenesis responses was first examined by growing plants in air from seed. This analysis revealed that the *cad2* mutation markedly affected the lesion formation that is spontaneously triggered in *cat2* in the absence of pathogen challenge and the associated induced resistance to subsequent bacterial challenge (Fig. 3). *PR* gene expression, which is spontaneously activated alongside lesion formation and bacterial resistance in *cat2*, was also decreased in *cat2 cad2* (Fig. 3). An effective block over H_2O_2-induced GSH accumulation and decreased lesion extent were also observed in double mutants carrying allelic mutations in the same GSH synthesis gene as *cad2* (Supplementary Fig. S1). The decrease in lesion extent was in good agreement with the severity in GSH deficiency, with *rax1*, the weakest mutation, producing a slightly weaker effect than *cad2* or *pad2* (Supplementary Fig. S1). In contrast to their effects on H_2O_2-triggered lesion extent, none of the secondary mutations reverted the decreased rosette size in *cat2* (Supplementary Fig. S1). Thus, blocking H_2O_2-triggered up-regulation of GSH deficiency led to down-regulation of lesion spread without producing general effects on the *cat2* oxidative stress phenotype. Of the three alleles, *cad2* is the best characterized and is intermediate in its effects on GSH contents (42; Supplementary Fig. S1). Due to this, the *cat2 cad2* line was chosen for a detailed examination of the processes underlying the role of GSH in linking intracellular H_2O_2 to induction of pathogenesis responses. The specific questions we sought to answer were: How is the effect of blocking GSH accumulation related to an antioxidant function? How is it related to the SA pathway and/or NPR1 function?

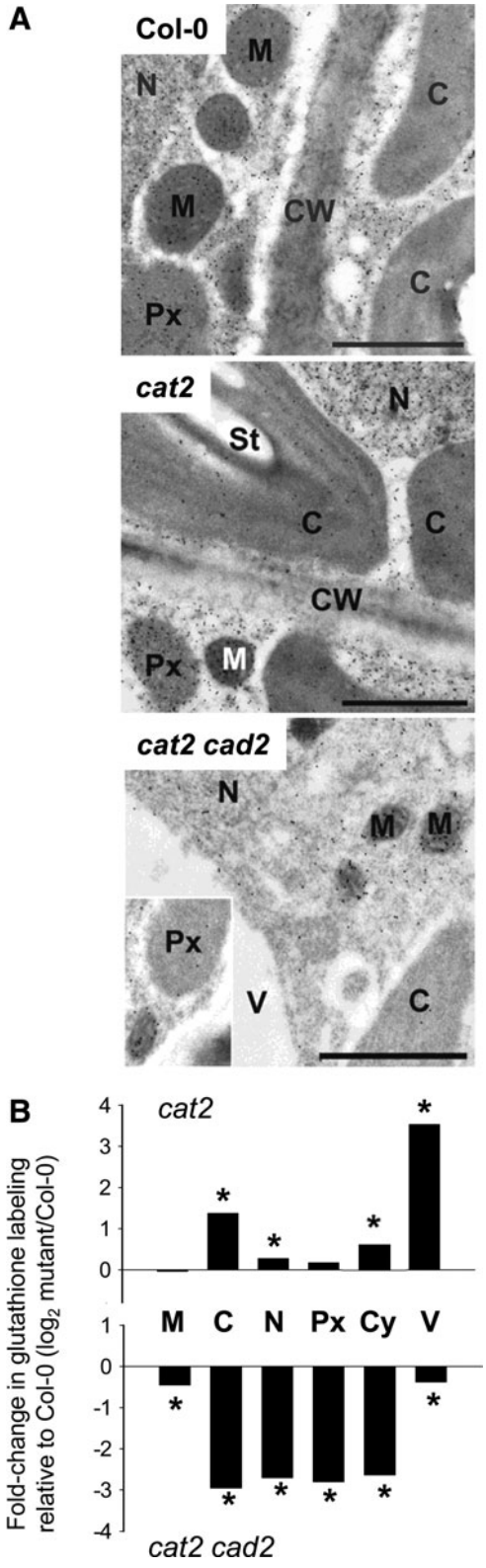

FIG. 2. Effects of the *cad2* mutation on subcellular distribution of GSH in response to oxidative stress. (A) Transmission electron micrographs showing subcellular distribution of gold-labeled GSH in photosynthetic mesophyll cells of Col-0, *cat2*, and *cat2 cad2*. The bars indicate 1 μm. **(B)** Relative quantitation of GSH labeling in different subcellular compartments. Plants were grown as described for Figure 1. Values show log fold change compared with Col-0. C, chloroplast; CW, cell wall; Cy, cytosol; M, mitochondria; N, nucleus; Px, peroxisome; St, starch; V, vacuole. *Significant difference from Col-0 at $p < 0.05$.

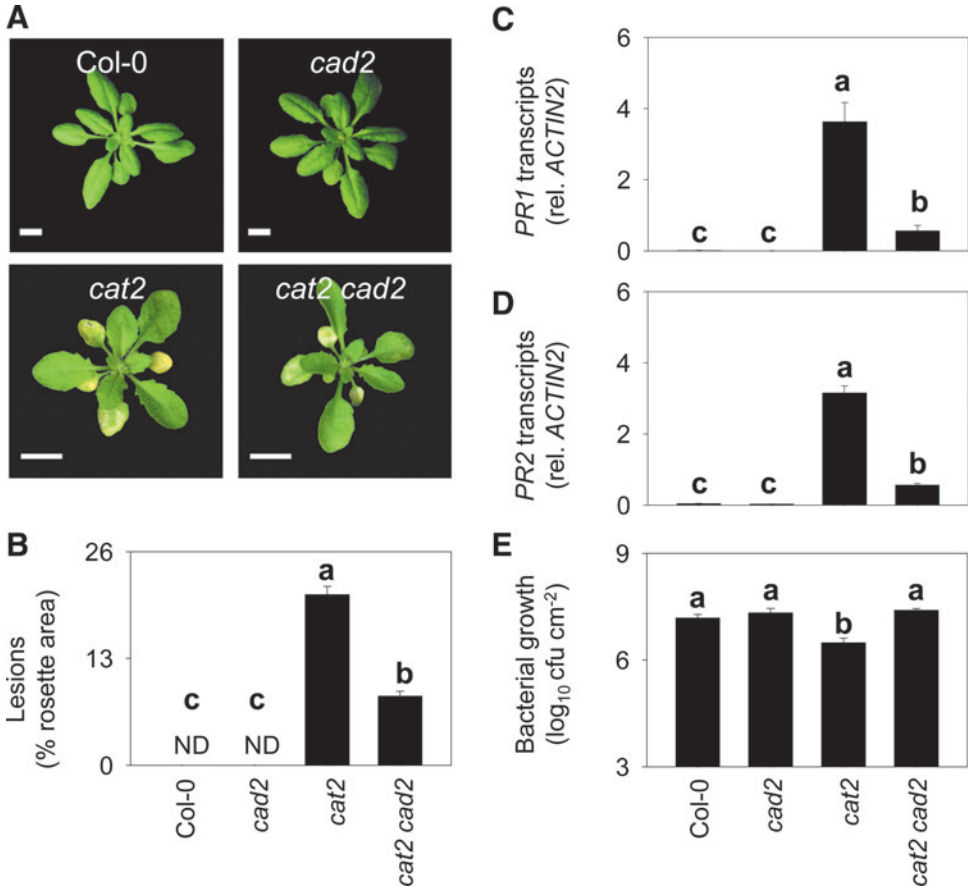

FIG. 3. Effect of the secondary *cad2* mutation on *cat2*-induced phenotype, *PR* gene expression, and bacterial resistance. (A) Phenotype of plants grown in air from seed. Photographs and samples were taken 21 days after sowing. Bars indicate 1 cm. **(B)** Lesion quantification in the different genotypes as a percentage of the total rosette area. ND, not detected. Values are means ± SE of at least 12 plants as in **(A)**. **(C)** and **(D)** *PR* transcripts quantified by quantitative polymerase chain reaction in the four genotypes, plants as in **(A)**. **(E)** Growth of virulent *Pseudomonas syringae* DC3000 in the four genotypes. *PR* transcripts show means ± SE of three biological replicates. Bacterial growth, means ± SE of four to six biological replicates. Different letters indicate significant difference at $p < 0.05$. ND, not detected. (To see this illustration in color, the reader is referred to the web version of this article at www.liebertpub.com/ars.)

Contrasting responses in cat2 cad2 and cat2 gr1 reveal a nonantioxidant role for GSH in coupling H_2O_2 to SA-dependent pathogenesis responses

Spreading lesions and associated responses in *cat2* can be abolished by introducing the *sid2* mutation (9). To check whether the decreased lesion extent in *cat2 cad2* occurs through the same ICS1-dependent pathway, we produced a *cat2 cad2 sid2* triple mutant. Growth of *cat2* backgrounds under conditions promoting lesion formation in *cat2* (continuous oxidative stress in air) revealed that, similar to *cat2 sid2*, *cat2 cad2 sid2* showed no detectable lesion formation (Supplementary Fig. S2).

Since partial GSH deficiency does not affect growth or biomass production in the *cat2* mutant, effects of the *cad2* mutation on *cat2* responses do not seem to be related to changes in oxidative stress intensity. To test this possibility further, we compared *cat2 cad2* phenotypes and SA dependency with those observed in *cat2 gr1*, in which loss of *GR1* function exacerbates oxidative stress in *cat2*, as reflected by an extreme dwarf phenotype and dramatic accumulation of oxidized GSH (36). To analyze the dependence of responses on SA and GSH accumulation, the *sid2* and *cad2* mutations were introduced into *cat2 gr1*.

To enable a meaningful comparison of the interactions between the different mutations, plants were initially grown at high CO_2, where the *cat2* mutation is silent. In this condition, *cat2*-dependent phenotypes and, in particular, the extreme phenotype of *cat2 gr1*, are annulled. Accordingly, in high CO_2 growth conditions, no phenotypic difference was observed between any of the lines (data not shown). After transferring plants to air, the phenotypes of *sid2*, *gr1*, and *cad2* were indistinguishable from Col-0, and none of these four genotypes presented lesions on the leaves (Supplementary Fig. S3). In contrast, the *cat2* mutation induced lesions that first became visible after 5 to 6 days, spreading to become very apparent after 10 days in air (Fig. 4A). Similar to its effects on *cat2* grown in air from seed, the *cad2* mutation restricted lesion spread, while the *sid2* mutation abolished it completely so that no lesions were visible in either *cat2 sid2* or *cad2 cad2 sid2* (Fig. 4A). All lines in which both *cat2* and *gr1* were present showed rapid onset of leaf bleaching, which was severe after 4 days exposure to air, irrespective of whether or not the *sid2* or *cad2* mutations were additionally present (Fig. 4A). Unlike the more slowly forming, persistent lesions observed in *cat2* and, residually, in *cat2 cad2*, the phenotypes of *cat2 gr1* backgrounds were transient, and the bleaching had largely disappeared within 10 days after transfer to air (Fig. 4A). Although *cat2 gr1* and *cat2 gr1 sid2* dramatically accumulated oxidized GSH, the phenotype induced by the combination of *cat2* and *gr1* mutations did not require this accumulation: Introduction of the *cad2* mutation into *cat2 gr1* restricted GSH contents well below *cat2* levels, yet reversible leaf bleaching was still observed (Figs 4A, B). Thus, the rapid-onset bleaching associated with loss of GSH recycling capacity appears to be associated with an antioxidant function rather than GSH status *per se* and does not require ICS1-dependent SA accumulation. This phenotypic response is, therefore, quite distinct from that produced by modulating GSH status through the *cad2* mutation.

Several recent publications have implicated *myo*-inositol in SA-dependent responses (8, 15, 35). In *cat2*, decreases in

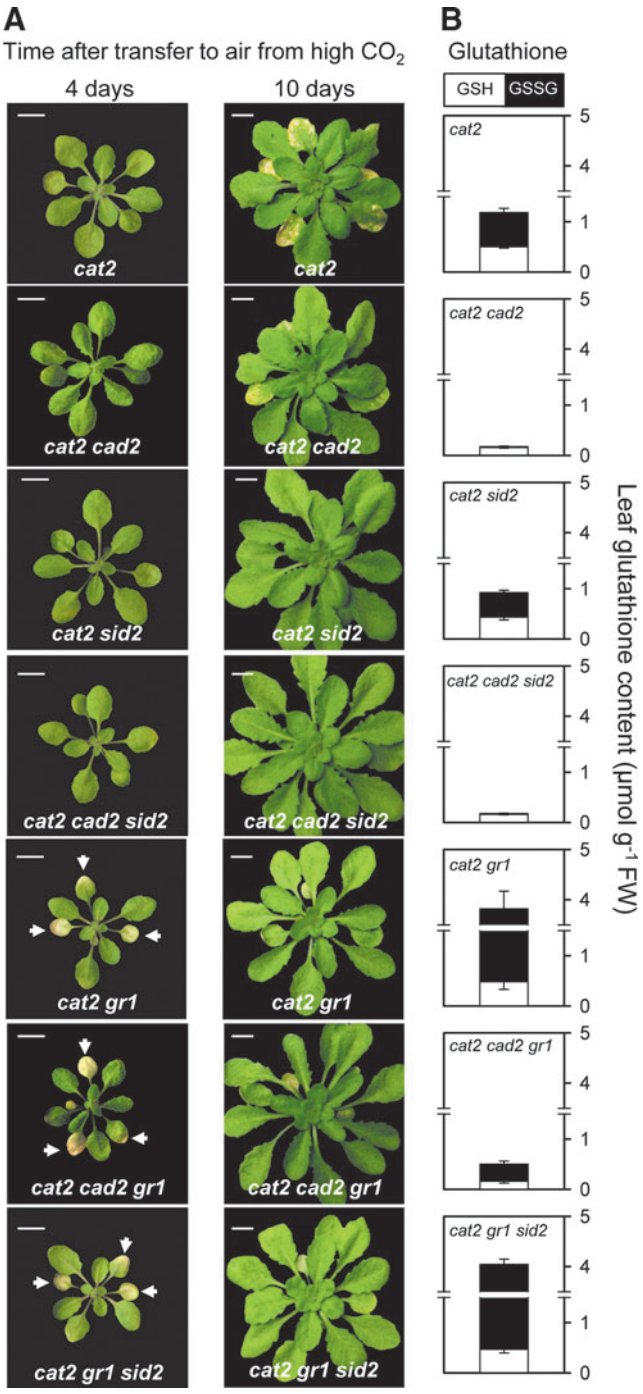

FIG. 4. Blocking GSH accumulation produces distinct effects on H_2O_2-triggered phenotypes to those produced by decreasing GSH-dependent antioxidative capacity. (A) Phenotypes in *cat2 cad2* and *cat2 gr1* induced by onset of oxidative stress in *cat2* and comparison with lines additionally carrying the *sid2* mutation in the SA synthesis pathway. Plants were grown for 3 weeks at high CO_2 and then transferred to air to induce oxidative stress in the *cat2* backgrounds. Photographs were taken 4 and 10 days after transfer of plants to air. Scale bars indicate 1 cm. Bleaching in *gr1* genotypes is indicated by *arrowheads*. **(B)** Leaf GSH contents in the different lines. White bars, GSH. Black bars, glutathione disulfide (GSSG). Values are means ± SE of 3 plants, sampled 4 days after transfer to air. (To see this illustration in color, the reader is referred to the web version of this article at www.liebertpub.com/ars.)

myo-inositol occur before SA accumulation and are necessary for induction of SA-dependent responses, as these can be prevented simply by treatment with exogenous *myo*-inositol (8). In both *cat2* and *cat2 cad2*, 4 days after transfer from high CO_2 to air, *myo*-inositol was decreased, and this was associated with decreases in galactinol, which is a product of *myo*-inositol (Supplementary Fig. S4). In contrast, the bleaching phenotype of *cat2 gr1* and *cat2 gr1 cad2* was associated with much less marked effects on these compounds. These

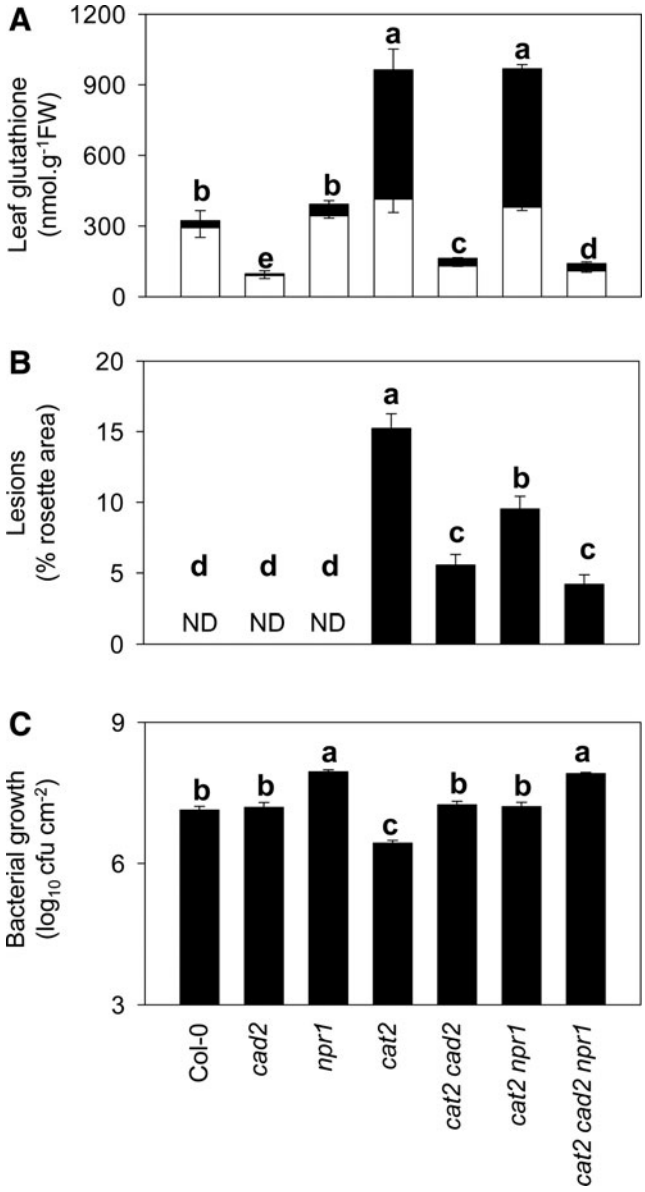

FIG. 5. Comparison of lesions, GSH contents, and bacterial resistance in *cat2 cad2* and *cat2 npr1*. (A) Leaf GSH contents. White bars, GSH. Black bars, GSSG. Values are means ± SE of 3 plants. **(B)** Lesion quantification as a percentage of the total rosette area. ND, not detected. Values are means ± SE of at least 12 plants. **(C)** Growth of virulent *P. syringae* DC3000 in all seven genotypes. Plants were grown at high CO_2 for 3 weeks to prevent any *cat2* phenotype, and inoculations were performed on plants 7 days after transfer to air to induce oxidative stress in *cat2* backgrounds. No difference in bacterial growth was observed between the genotypes at 0 hpi.

observations provide further evidence (1) that *myo*-inositol metabolism is important in linking intracellular H_2O_2 to downstream SA responses, and (2) that loss of GSH antioxidant recycling function entrains an SA-independent stress response which is distinct from the SA-dependent pathway operating in *cat2* and *cat2 cad2*.

Side-by-side comparison of cat2 cad2 with cat2 npr1

To establish whether the effect of GSH deficiency on pathogenesis responses in *cat2* is related to impaired NPR1 function, double *cat2 npr1* mutants were produced and analyzed in parallel with *cat2 cad2*. The *npr1* mutation did not affect GSH status in either Col-0 or *cat2* backgrounds (Fig. 5A). It did, however, decrease lesion formation in *cat2*, though less markedly than did *cad2* (Fig. 5B and Supplementary Fig. S5). The triple *cat2 cad2 npr1* line showed similar GSH contents and lesion formation to those observed in *cat2 cad2* (Fig. 5). Thus, H_2O_2-induced alterations in GSH status were independent of the presence or absence of functional NPR1 in both *cat2* and *cat2 cad2* backgrounds. None of the mutations affected bacterial growth sampled immediately after inoculation (data not shown), but clear differences were observed in growth in samples taken at two days postinoculation (Fig. 5C). Similar to *cad2*, *npr1* annulled *cat2*-induced resistance: both *cat2 cad2* and *cat2 npr1* showed Col-0 resistance levels (Fig. 5C). However, *cat2 npr1* still showed higher resistance than *npr1*.

In a first approach that analyzed whether the effects of blocking GSH up-regulation were linked to impaired NPR1 function, comparative gas chromatography-time of flight-mass spectrometry (GC-TOF-MS) analysis of the two double mutants was performed (Supplementary Table S1). By generating information on about 100 different compounds, this technique produces a metabolic signature for intracellular oxidative stress in *cat2*, which shows substantial overlap with that induced by bacterial pathogens (10). A key feature of the *cat2* metabolic signature is accumulation of a wide range of metabolites in an SA-dependent fashion, that is, most of the signature is annulled in *cat2 sid2* double mutants (9).

Both *cad2* and *npr1* mutations affected *cat2*-triggered metabolite profiles, but in very different ways (Fig. 6A). Comparison of the profiles shown in Figure 6A with those previously described for *cat2 sid2* sampled in the same conditions revealed that *cat2 npr1* and *cat2 cad2* recapitulated different parts of the *cat2 sid2* profile (Fig. 6B). For this comparative analysis, we included only metabolites that were detected in both the earlier study of *cat2 sid2* (9) and the present one. For example, 17 metabolites were significantly different from *cat2* in *cat2 npr1* (Supplementary Table S2), but only 11 of these were also detected in our previous study. Of these 11, the *sid2* and *npr1* mutations significantly affected eight in the same direction (Fig. 6B, middle). Using the same approach, only two metabolites that were detected in this study and our earlier one (gluconic acid and threonine) were affected similarly by the *cad2* and *npr1* mutations in the *cat2* background. These two compounds are among those strongly induced in *cat2* and in response to bacterial infection (10), and the induction of both was significantly decreased by *sid2*, *cad2*, or *npr1* mutations (Fig. 6B). Six other metabolites were affected similarly in *cat2 sid2* and *cat2 npr1* (Fig. 6B, middle), whereas the response of seven metabolites in *cat2* was unaffected by *npr1* but decreased by both *cad2* and *sid2* mutations (Fig. 6B, top). These seven compounds included several metabolites associated with pathogenesis responses, including tryptophan, putrescine, and the glucosylated form of SA.

Targeted quantification of free and total SA by HPLC showed that both accumulated in *cat2* and that their accumulation was markedly enhanced by the *npr1* mutation (Fig. 7A). In *cat2 npr1*, total SA accumulated to thrice the values in *cat2*. This hyper-accumulation of SA is consistent with effects of the *npr1* mutation in other mutants showing constitutive induction of SA-dependent pathogenesis responses (55, 71). In marked contrast to the effect of *npr1*, the *cad2* mutation substantially decreased SA accumulation (Fig. 7A). SA levels in the triple *cat2 cad2 npr1* mutant were similar to those in the *cat2* single mutant (Fig. 7A). Thus, the *cad2* mutation decreased SA accumulation in both the *cat2* and *cat2 npr1* backgrounds, providing further evidence that the principal effect of GSH deficiency on H_2O_2-triggered pathogenesis responses is mediated *via* a different route than impairment of NPR1 function.

Due to the decreased SA accumulation in *cat2 cad2*, we analyzed expression of *ICS1*, the key enzyme in the production of SA in response to pathogens (66), during continuous growth of plants in air from seed. *ICS1* expression showed a marked transient increase in *cat2* (Fig. 7B), with the initial increase correlating with the onset of lesions, which begin to be visible after about 16 days of growth. The induction of *ICS1* was strongly damped in *cat2 cad2* (Fig. 7B), in agreement with the decreased lesions (Fig. 3) and SA contents (Fig. 7A).

Complementation experiments reveal nonredundant roles for GSH and NPR1 in the activation of SA-dependent responses

Experiments in which SA content and *ICS1* and *PR1* transcripts were quantified after transfer to high CO_2 following previous growth in air confirmed that both were significantly less accumulated in *cat2 cad2* compared with *cat2* (Fig. 8A, B). To examine whether SA accumulation in *cat2 cad2* could be restored by glutathione, plants were treated with GSH or

FIG. 6. GC-TOF-MS analysis of the impact of *cad2* and *npr1* mutations on H_2O_2-dependent metabolite profiles. (A) Heat map showing hierarchical clustering of all detected metabolites. Values were centered reduced before clustering analysis. **(B)** Comparison of metabolite profiles in *cat2 cad2* and *cat2 npr1* with those previously reported for *cat2 sid2* (9). The values in the Venn diagrams indicate the number of metabolites that were significantly different in each double mutant relative to *cat2*. Overlapping sections indicate the number of metabolites that showed same-direction significant effects in *cat2 sid2* and *cat2 cad2* (top), *cat2 sid2* and *cat2 npr1* (middle), and *cat2 cad2* and *cat2 npr1* (bottom). For each comparison, the graphs show values (normalized to *cat2*) plotted for common metabolites, with left and right bars of each pair showing the genotypes indicated to the left and right, respectively, of the Venn diagram above each graph. Gluconic acid and threonine were the only two compounds affected similarly by all three secondary mutations. Plants were grown from seed in air in long days and sampled 23 days after sowing. Three biological repeats were analyzed for each genotype. For a full list of metabolites and statistical analysis, see Supplementary Table S2. (To see this illustration in color, the reader is referred to the web version of this article at www.liebertpub.com/ars.)

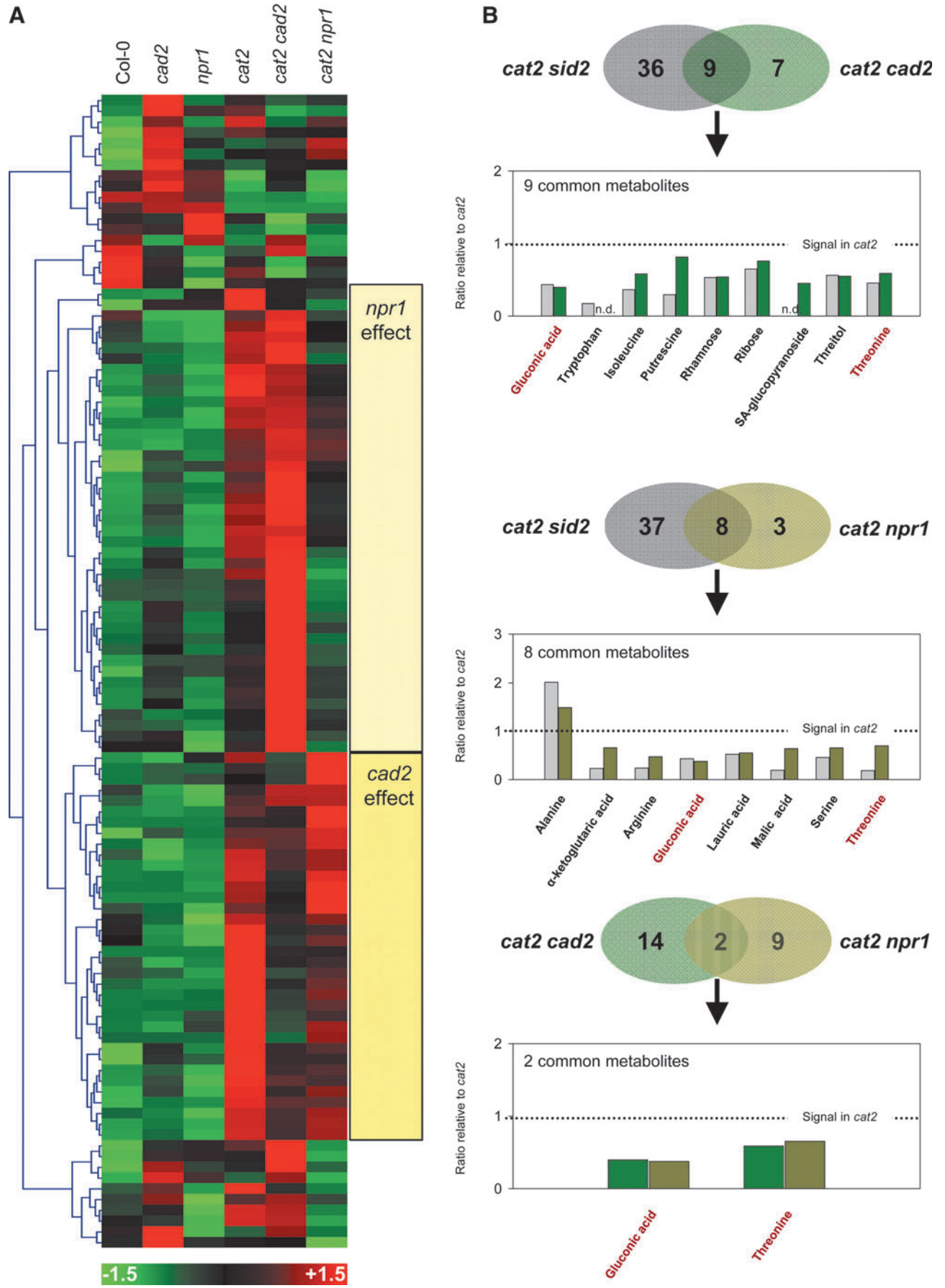
A
Col-0
cad2
npr1
cat2
cat2 cad2
cat2 npr1
npr1 effect
cad2 effect
-1.5
+1.5
B
cat2 sid2
36
9
7
cat2 cad2
9 common metabolites
Signal in cat2
Ratio relative to cat2
n.d.
Gluconic acid
Tryptophan
Isoleucine
Putrescine
Rhamnose
Ribose
SA-glucopyranoside
Threitol
Threonine
cat2 sid2
37
8
3
cat2 npr1
8 common metabolites
Alanine
α-ketoglutaric acid
Arginine
Gluconic acid
Lauric acid
Malic acid
Serine
Threonine
cat2 cad2
14
2
9
cat2 npr1
2 common metabolites
Gluconic acid
Threonine

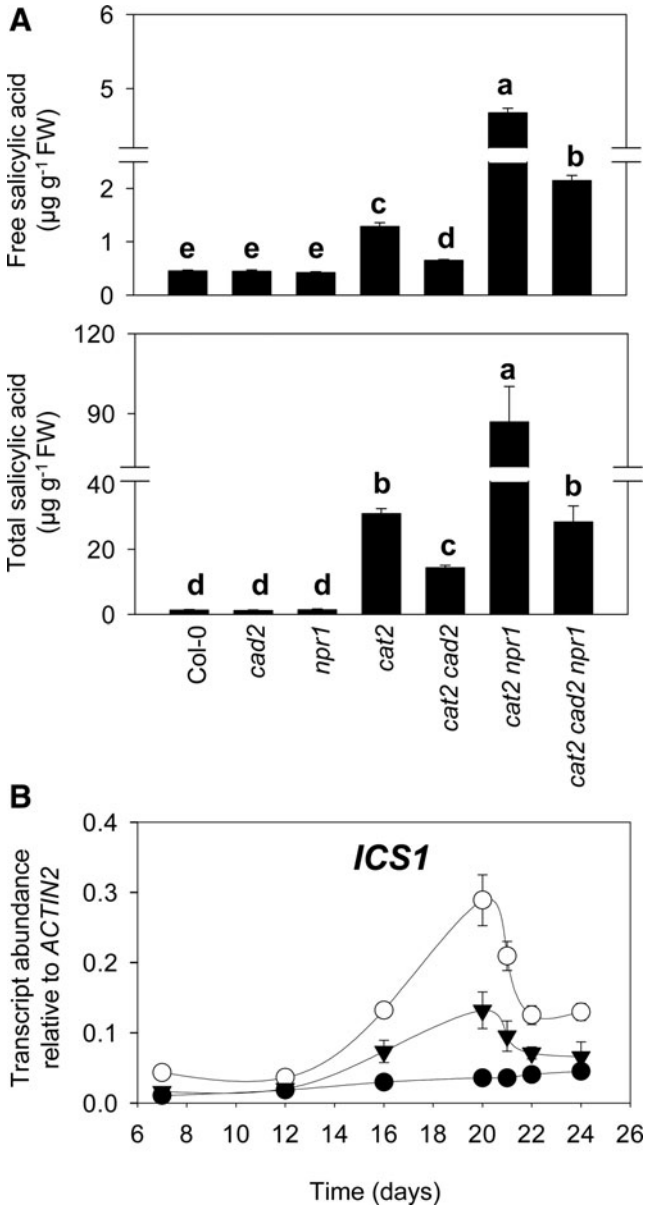

FIG. 7. Analysis of salicylic acid (SA) and *ICS1* transcripts in double and triple mutants. (A) Free and total SA in *cat2*, *cad2*, *npr1*, and double and triple mutants. Different letters indicate significant difference at $p < 0.05$. Plants were grown in air, and samples were taken 21 days after sowing. **(B)** Time course of *ICS1* transcript levels in Col-0 (black circles), *cat2* (white circles), and *cat2 cad2* (triangles). Plants were grown as in **(A)**. Time indicates days after sowing. All values are means ± SE of three biological replicates.

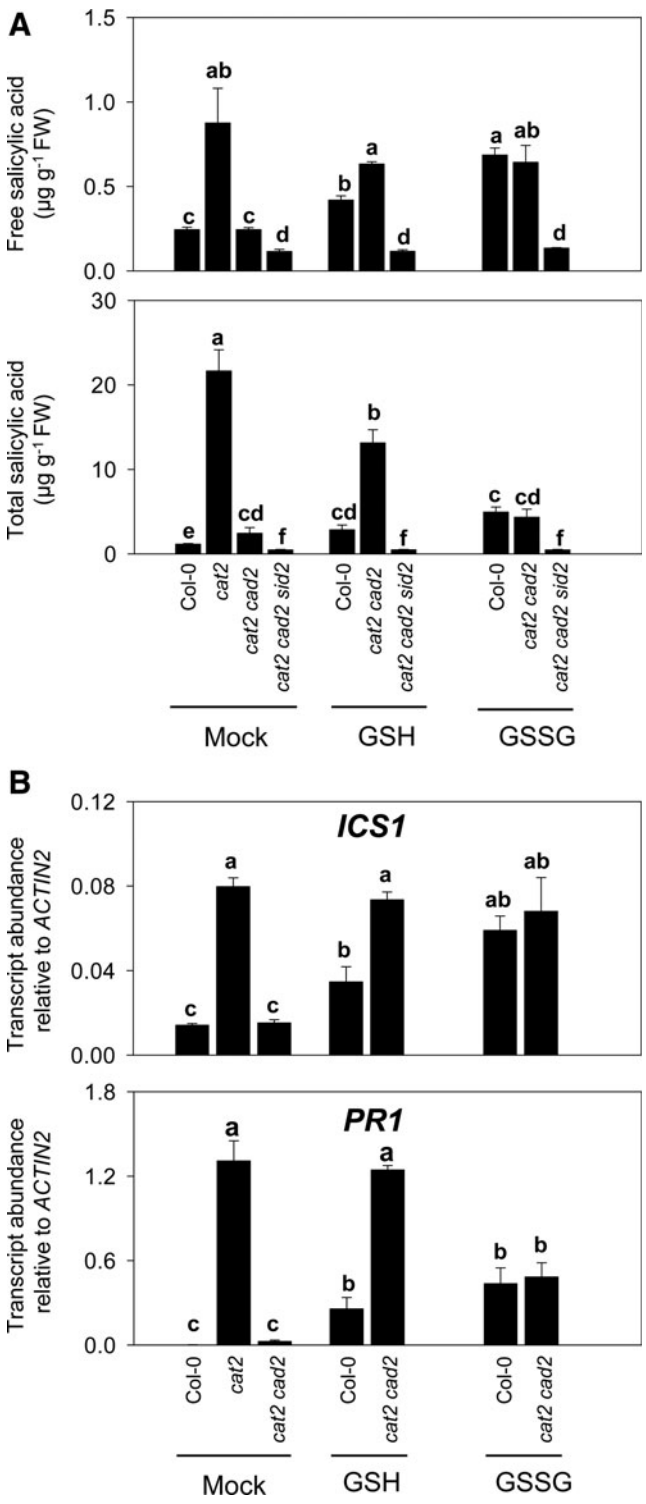

FIG. 8. Glutathione complementation of SA accumulation and related gene expression in *cat2 cad2*. Plants were grown at high CO_2 for 3 weeks to prevent any *cat2* phenotype, then transferred to air to induce oxidative stress in *cat2* backgrounds. From the first day after transfer to air, rosettes were treated once daily by spraying with water, 1 m*M* GSH, or 1 m*M* GSSG. Samples were taken after 9 days. **(A)** Free and total SA contents in Col-0, *cat2*, *cat2 cad2*, and *cat2 cad2 sid2*. **(B)** *ICS1* and *PR1* expression in Col-0, *cat2*, and *cat2 cad2*. Values are means ± SE of 3 biological replicates. Different letters indicate significant difference at $p < 0.05$.

GSSG. Both forms induced SA above basal levels in Col-0, with GSSG being the more effective of the two (Fig. 8A). In *cat2 cad2*, in which the *cat2* mutation should activate H_2O_2 signaling, GSH was most effective, restoring total SA to about 60% of *cat2* levels (Fig. 8A). This effect was not observed in *cat2 cad2 sid2*, showing that it was dependent on functional ICS1. We, therefore, investigated the effects of GSH supplementation on *ICS1* expression. Restoration of SA accumulation in *cat2 cad2* by added GSH was associated with enhanced induction of both *ICS1* and *PR1* genes (Fig. 8B). Further, GSSG

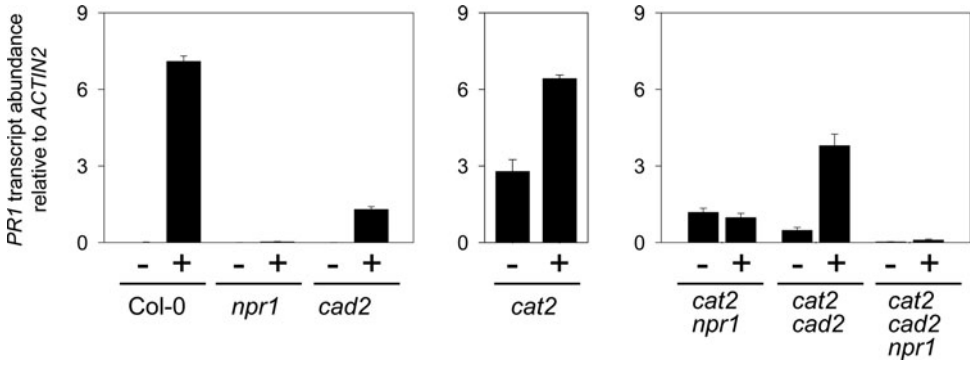

FIG. 9. Comparison of *PR1* inducibility by SA in *npr1, cad2, cat2,* and double and triple mutants. Plants were grown in air from seed for 20 days after sowing and then sprayed either (−) with water (mock) or (+) with 0.5 m*M* SA, and samples were taken 24 h later. Values are means ± SE of three biological replicates.

effectively induced *ICS1*, even in the absence of an H_2O_2 signal (Col-0), although GSSG was much less effective than GSH in inducing *PR1*. The GSH treatments also promoted lesion formation in *cat2 cad2* (data not shown).

To establish whether down-regulation of SA-dependent responses in *cat2 cad2* was linked to attenuated SA accumulation or impaired NPR1 function, the effects of SA supplementation on *PR1* expression were examined in the different lines. In Col-0, *npr1*, and *cad2*, *PR1* expression was very low in the absence of added SA (Fig. 9). SA treatment strongly induced *PR1* in Col-0 but not significantly in *npr1*. In *cad2*, SA was able to induce *PR1* but to lower levels than in Col-0 (Fig. 9). SA treatment of *cat2* showed that *PR1*, already strongly induced in the absence of added SA, was induced a further 2-fold (Fig. 9). In *cat2 npr1*, *PR1* was induced in the absence of SA, though to a lower level than in *cat2* (Fig. 9). This suggests that an NPR1-independent pathway of *PR* gene induction can operate in the *cat2 npr1* background, as previously reported during SA-dependent interactions with certain pathogens (30, 48, 54). While SA was unable to further induce *PR1* in *cat2 npr1*, *PR1* was induced by SA about 8-fold in *cat2 cad2*, so that transcripts were intermediate between *cat2*–SA and *cat2* + SA (Fig. 9).

Discussion

A substantial body of work shows that GSH is a multifunctional metabolite with diverse functions in plant defense and antioxidative metabolism. Since signaling roles of GSH might be mediated by several types of reactions, many of which could be dependent on functionally redundant proteins encoded by quite large gene families, establishing the role of specific GSH-dependent components is a formidable task. In this study, we investigated the role of GSH-dependent processes in H_2O_2 signaling by seeking to genetically abrogate oxidation-triggered accumulation of GSH.

Partial impairment of γ-glutamylcysteine synthetase function confers a genetic block on H_2O_2-triggered up-regulation of GSH

The *cad2*, *rax1*, and *pad2* mutations in the single gene encoding the first committed enzyme of glutathione synthesis (γ-glutamylcysteine synthetase [γ-ECS]) produce constitutive partial decreases in GSH (3, 11, 42). Here, we show that these mutations also block H_2O_2-triggered up-regulation of GSH. In Arabidopsis, the γ-ECS protein is located in the chloroplast (65). There is little evidence that accumulation of GSH in *cat2* is linked to enhanced synthesis of γ-ECS protein (46). Based on current knowledge, the major player is post-translational activation of γ-ECS by disulfide bond formation (22, 23). However, the factors that mediate oxidation of γ-ECS thiols *in vivo* remain to be identified. Unlike the wild-type enzyme present in *cat2*, the mutant γ-ECS does not appear to be oxidatively activated in *cat2 cad2*. However, in *cat2 cad2*, GSH remained close to *cad2* values; whereas in *cat2 gr1*, GSH accumulated to much higher levels than in *cat2* (Fig. 4). Thus, GSH stayed highly reduced and below Col-0 levels in *cat2 cad2*, while a highly oxidized GSH pool in *cat2 gr1* was associated with dramatic accumulation. These observations are consistent with a satisfyingly simple model for γ-ECS regulation in which GSSG produced from GSH oxidation allows activation of the enzyme to up-regulate GSH synthesis. This receives support from GSH contents in *cat2 cad2 gr1*, which were intermediate between *cat2 cad2* and *cat2* (Fig. 4). Indeed, the chloroplast was among the cellular compartments that showed the highest H_2O_2-triggered GSH accumulation in *cat2* (Table 1). Since the accumulated GSH in *cat2* is almost all in the disulfide form (Figs 1 and 5), it is highly likely that in *cat2* the chloroplast is enriched in GSSG but that this enrichment does not occur in *cat2 cad2*.

In all three double mutants blocked in GSH accumulation, including *cat2 rax1* carrying the weakest allele, the overall leaf GSH pool remains highly reduced in conditions that permit increased H_2O_2 availability (Supplementary Fig. S1). In *cat2 cad2 gr1*, a limited accumulation of GSH was accompanied by significant oxidation relative to *cat2 cad2* (Fig. 4). From a cellular point of view, these striking observations suggest that the plant cell GSH redox system is configured so that not only oxidation drives enhanced accumulation of total GSH but also decreased contents inhibit GSH oxidation. This two-way interaction may be important in setting appropriate conditions for cellular signaling. The underlying factors remain unclear but could include, for example, affinities of the enzymes that oxidize GSH to GSSG or the differences in GSH compartmentation in *cat2* and *cat2 cad2*. Whatever the underlying causes, GSH contents are known to change during development (43) and in response to factors such as sulfur nutrition (39). A strong interplay between concentration and redox state could influence the outcome of redox-dependent responses to external stresses in different circumstances.

An essential role for GSH in activation of H_2O_2-dependent SA signaling and related pathogenesis responses

Alongside up-regulation of GSH, the *cat2* mutation induces SA and a wide range of SA-dependent responses in an ICS1-

dependent manner (9). Using nontargeted metabolite profiling and targeted analysis of recognized defense compounds, we recently reported that SA-dependent responses triggered by intracellular H_2O_2 in *cat2* show considerable similarity with responses to pathogenic bacteria (10). Thus, intracellular H_2O_2 generated by the peroxisome-located photorespiratory glycolate oxidase closely mimics redox processes involved in biotic stress. Several studies suggest that down-regulation of CAT plays some role in pathogenesis responses (37, 64), while the analysis of glycolate oxidase mutants provides further indications of roles for peroxisomally produced H_2O_2 in pathogenesis responses (51). The potential relevance of redox-triggered events in *cat2* is underscored by effects observed in double mutants in which *cat2* responses are modulated by loss of function of recognized players in pathogenesis (9, 10). The present study provides direct evidence that GSH is a key player linking increased H_2O_2 to downstream phytohormone signaling. Blocking up-regulation of GSH in *cat2* antagonizes H_2O_2-triggered SA accumulation, expression of SA-dependent marker genes, and induced resistance to bacteria.

The residual SA-linked responses in *cat2 cad2* are completely annulled in *cat2 cad2 sid2*, suggesting that GSH status modulates the efficiency of H_2O_2-triggered signaling through the ICS1-dependent pathway. This conclusion is supported by the attenuated induction of the *ICS1* gene in *cat2 cad2* compared with *cat2* (Fig. 7). Similar to γ-ECS, ICS1 is a chloroplast enzyme that could potentially be redox regulated. However, post-translational control of ICS1 by thiol-disulfide status has been discounted on the basis of the protein's structural features (58). Our data reveal that the expression of *ICS1* may be under redox regulation through GSH-dependent processes downstream of H_2O_2. The intermediates in this signaling pathway remain to be identified.

GSH acts independently of its antioxidant function in transmitting H_2O_2 signals

A central premise of this study was that H_2O_2-triggered modulation of GSH (as a result of the antioxidant function of GSH) might be perceived by the cell as a signal. To test this hypothesis, we sought to manipulate GSH status in an H_2O_2 signaling system, without affecting overall cellular antioxidant capacity. That the block over GSH up-regulation in *cat2 cad2* and allelic lines achieves this objective is evidenced by the following observations. First, introduction of *pad2*, *cad2*, or *rax1* mutations does not affect the oxidative stress-dependent decreased growth phenotype of *cat2.* Second, the block over H_2O_2-triggered GSH accumulation in *cat2 cad2* is quite specific, and not accompanied by increased oxidation of ascorbate or NADPH, or by enhanced accumulation of peroxides. Third, blocking the GSH synthesis pathway decreases rather than increases *cat2*-dependent lesion spread. Fourth, and most crucially, the ICS1-linked effects observed in *cat2 cad2* are quite distinct from the responses to exacerbated oxidative stress produced by knocking out both *CAT2* and *GR1*.

In addition to the ICS1-independent phenotypes of *cat2 gr1*, the contrasting effects of *cad2* and *gr1* mutations on the *cat2* response are underscored by analysis of metabolite markers for the SA-dependent pathway. Entrainment of SA-dependent responses in *cat2* requires decreased *myo*-inositol (8). In *cat2 cad2*, as in *cat2*, this compound and the related metabolite galactinol were decreased (Supplementary Fig. S4), even though the *cat2*-triggered SA response was attenuated in the double mutant. This indicates that GSH status exerts its effects on the SA pathway downstream of *myo*-inositol. Together with our earlier analysis, it suggests a model in which H_2O_2 decreases *myo*-inositol concentrations, an effect that then allows SA accumulation through GSH -dependent processes. Despite the enhanced oxidative stress in *cat2 gr1* and *cat2 cad2 gr1*, both these compounds remained at levels close to wild type, suggesting that decreases in *myo*-inositol are not simply related to oxidative stress intensity.

Together, these data further illustrate that SA-dependent lesions in *cat2* are not a simple consequence of oxidative stress intensity. Rather, they are the result of an H_2O_2-initiated programmed response whose intensity is modulated by GSH. Elucidation of events underlying the intriguing reversibility of the SA-independent phenotypes in *cat2 gr1* backgrounds will require further study, although it is perhaps worth noting that Arabidopsis lines deficient in both CAT2 and APX1 show induction of novel protective mechanisms that are not observed in lines deficient in only CAT2 or APX1 (63). Failure of *cat2 gr1* to induce the SA-dependent phenotype observed in *cat2* perhaps suggests that an optimal level of oxidation is required to entrain effective induction of pathogenesis responses. Beyond a certain threshold intensity, SA-dependent pathogenesis program is no longer activated. Thus, even when triggered by a single type of ROS (H_2O_2 in this study), intracellular oxidative stress can drive several distinct phenotypic outcomes.

GSH can regulate SA signaling through processes additional to NPR1

NPR1 is, by far, the best-characterized thiol-dependent protein involved in pathogenesis responses, and can be activated by GSH addition to cells or leaves (20, 38). Both pathogens and SA can cause adjustments in leaf GSH pools (17, 26, 32, 34, 62). However, the precise nature of the redox factors controlling NPR1 *in vivo* is still open to debate. While *h*-type thioredoxins, which are known to be induced during pathogenesis responses (27), were shown to perform the reductive activating step (59), a recent study has revealed the complexity of NPR1 regulation (29).

Apart from abolishing H_2O_2-triggered increases in chloroplast GSH, the *cad2* mutation prevented increases in cytosolic and nuclear concentrations (Fig. 2 and Table 1). Based on current knowledge, this effect might be predicted to compromise NPR1 function. Indeed, the NPR1 pathway is clearly functional in *cat2*, as the *npr1* mutation produced the following effects in *cat2 npr1*: impaired lesion spread relative to *cat2*, partial loss of *PR* gene expression, a complete loss of *PR1* inducibility by exogenous SA, and a characteristic metabolite signature, including hyper-accumulation of SA. Consistent with previous studies of plants with altered cytosolic GSH status (33), exogenous SA induced *PR1* less effectively in *cad2* than in Col-0. However, if the effect of the *cad2* mutation on *cat2* responses occurred exclusively through partial or complete loss of NPR1 function, we would predict that *cat2 cad2* should show same-direction responses to *cat2 npr1*. In fact, of the *cat2 npr1* features listed earlier, the only one shared by *cat2 cad2* was decreased lesion spread relative to *cat2*. *PR1*

expression was even lower in *cat2 cad2* than in *cat2 npr1* and was inducible by exogenous SA. Crucially, blocking GSH accumulation in *cat2 cad2* produced a metabolite signature that was distinct from that observed in *cat2 npr1*. These distinct effects were most striking for SA contents: If effects of the *cad2* mutation were purely explainable in terms of loss of NPR1 function, *cat2 cad2* should be expected to have higher SA contents than *cat2* (as in *cat2 npr1*). In fact, we observed the opposite. Thus, it seems that GSH plays a regulatory role in SA signaling additional to NPR1. Indeed, the similar GSH status in *cat2* and *cat2 npr1* provides little evidence for feedback between NPR1 and GSH.

Hyper-accumulation of SA in *cat2 npr1* was associated with H_2O_2-triggered NPR1-independent *PR1* expression and bacterial resistance. The operation of this NPR1-independent pathway seems itself to be dependent on GSH, because *cat2 cad2 npr1* similarly showed low resistance (Fig. 5C) and *PR1* expression to *npr1* (Fig. 9), showing that the *cad2* and *npr1* mutations act additively to annul part of the *cat2*-induced resistance responses. Again, this suggests that blocking upregulation of GSH impairs H_2O_2-triggered pathogenesis responses *via* effects that are distinct from those of the *npr1* mutation. A key difference between *cat2 npr1* and *cat2 npr1 cad2* is that the hyper-accumulation of SA in the former is not observed in the latter. Together with differences in SA accumulation in *cat2* and *cat2 cad2*, this suggests that GSH plays an important role in H_2O_2 signaling at the level of induction of SA itself.

Multifunctional roles of GSH status in defense signaling pathways: A model

The observations reported in this study reveal that H_2O_2-triggered changes in GSH status are not merely a passive response to oxidative stress. Rather, they suggest that modulation of GSH status is required to link increases in intracellular H_2O_2 production to activation of the ICS1-dependent SA pathway. This function would operate within the context of dynamic modulation of GSH that involves initial oxidation leading to downstream reduction during some pathogenesis responses (26, 38, 62). While a potential role for GSH in the reductive phase has been described at the level of NPR1, our report provides the first direct evidence that initial oxidative events necessary for SA accumulation require changes in GSH status. The down-regulation of the SA pathway in *cat2 cad2*, in which GSH stays highly reduced, suggests that these oxidative events involve a decrease in the GSH:GSSG ratio (Fig. 10). Failure to produce an appropriately oxidized GSH status would then inhibit initiation of the pathway, explaining our observation that introducing the *cad2* mutation antagonizes SA accumulation, *PR1* induction, and induced resistance in both *cat2* and *cat2 npr1* (Fig. 10). When GSH oxidation is accompanied by severe oxidative stress, as in *cat2 gr1* backgrounds, an alternative response to the SA pathway is entrained.

Both pathogenesis responses and GSH status are influenced by sulfur nutrition (24, 25). More generally, photoautotrophism means that redox modulation is a central player in linking energy and nutritional status to appropriate stress outcomes within the complex metabolic network and plastic developmental program of plants (18, 40). The key role of GSH status we report here may be relevant to understanding and optimizing pathogenesis responses in plants growing in natural environments with variable nutrition.

Materials and Methods

Plant material and mutant characterization

All the Arabidopsis mutants used in this study were in the Columbia genetic background, and their key features are summarized in Supplementary Table S1. The homozygous mutants were *cat2-1* (SALK_076998; 46), *cad2* (11), *gr1* (SALK_060425; 36), *npr1* (7), *rax1* (3), *pad2* (42), and *sid2* (66). The seeds of T-DNA insertion lines were obtained from the Nottingham Arabidopsis Stock Centre (http://nasc.nott.ac.uk), and homozygotes were identified using sequence information obtained from the SIGnAL Web site at http://signal.salk.edu. The *cat2 gr1* and *cat2 sid2* plants have been previously described in references (36) and (9), respectively. Four previously undescribed double and four previously

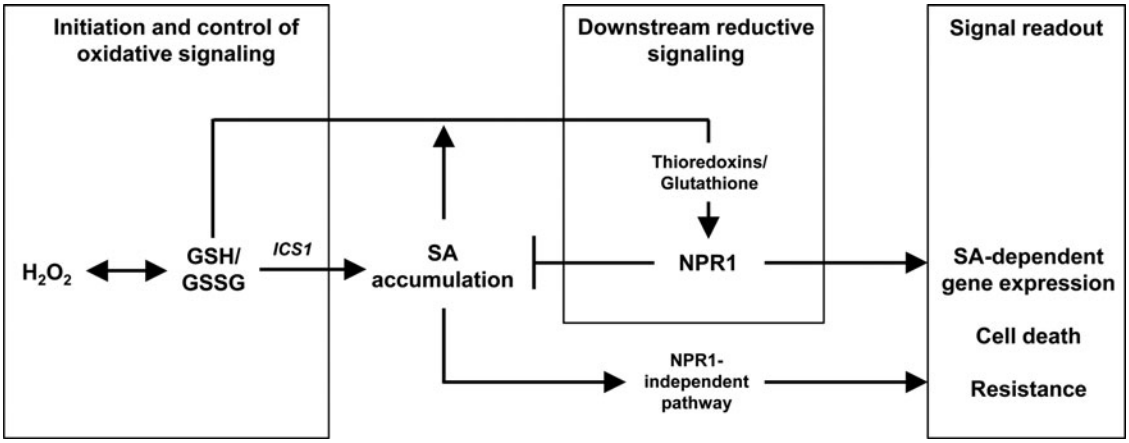

FIG. 10. Glutathione status is a key player linking intracellular H_2O_2 to activation of the SA pathway in *cat2*. Oxidation by H_2O_2 modulates GSH status. This oxidative modulation is a part of the signal network required for optimal ICS1-dependent SA accumulation that then leads to activation of NPR1 function through reductive processes (38), to which GSH may also contribute.

undescribed triple mutants were produced for this study: *cat2 cad2*, *cat2 npr1*, *cad2 pad2*, *cat2 rax1*, *cat2 cad2 sid2*, *cat2 cad2 npr1*, *cat2 cad2 gr1*, and *cat2 gr1 sid2* (Supplementary Fig. S6). For T-DNA insertions, leaf DNA was amplified by polymerase chain reaction (PCR) using primers specific for left borders and *CAT2* and *GR1* genes (Supplementary Table S3). The genotypes of F1, F2, and F3 progeny at the *SID2* locus were determined by *Tru9I* digestion of a 243-bp PCR fragment using specific primers (Supplementary Fig. S6). Zygosity of the *cad2* and *npr1* mutations was established using restriction length polymorphism based on *Bsl*I and *Nla*III, respectively (Supplementary Fig. S6).

Plant growth and sampling

Seeds were incubated for 2 days at 4°C and then sown on soil. Plants were grown in a controlled-environment growth chamber in a 16 h photoperiod and an irradiance of 200 μmol m^{-2} s^{-1} at leaf level, 20°C/18°C, 65% humidity, and given nutrient solution twice per week. The CO_2 concentration was maintained at 400 μL L^{-1} (air) or 3000 μL L^{-1} (high CO_2). Samples were rapidly frozen in liquid nitrogen and stored at −80°C until analysis. Unless otherwise stated, data are means ± SE of at least three independent samples from different plants.

Cytohistochemical analysis

Sample preparation for cytohistochemical investigations was performed as previously described in detail (47, 70). Immunolocalization of GSH was performed as previously described (69). Subcellular concentrations of GSH from immunogold labeling densities were estimated according to (47). Concentrations for each genotype were based on global leaf GSH + GSSG contents measured in Col-0, *cat2*, and *cat2 cad2*. The amount of GSH in each compartment (nmol g^{-1} FW) was obtained by multiplying the leaf GSH contents by the measured fractional contribution of each compartment to the overall gold label. From these values, concentrations were calculated using sub-cellular volumes estimated in leaf sections of each genotype. Measurements of the percentage volume for each compartment were estimated as in (47). Subcellular volumes for each cell compartment were finally calculated per g fresh weight from the percentage volumes based on a mesophyll volume per leaf mass of 773 μl.g^{-1} FW (68).

Lesion quantification and pathogen tests

Percentages of lesion areas were quantified using IQmaterials software. Growth of *Pseudomonas syringae* pv tomato strain DC3000 was assessed 48 h postinoculation as earlier (9). Three of the middle leaves on five to seven different plants of each genotype were inoculated using a 1-ml syringe without a needle with *Pst* DC3000 in a medium titer of 5×10^5 colony-forming units ml^{-1}. Leaf discs were taken for analysis either immediately (0 h) or 48 h later.

Metabolite and enzyme measurements

An enzymatic assay of NADP(H), ascorbate, and GSH was performed as previously described (43). Peroxides were measured by luminol luminescence (45). Free and total SA were measured by HPLC-fluorescence (9). Nontargeted metabolite profiling and relative quantification of *myo*-inositol and galactinol were performed by GC-TOF-MS on triplicate biological repeats (10). Compounds identified by retention index were confirmed by reference to mass spectra libraries. Peak area was quantified based on specific fragments and was corrected on the basis of an internal standard (ribitol) and sample fresh weight. For data display (Figure 6), values were centered reduced, that is, for each metabolite, mean and standard deviation values were produced across all samples. For each genotype, the mean value for metabolite "x" was subtracted from the mean across all samples (centered), and the resulting value was divided by the SD for that metabolite (reduced). Significant metabolites were identified by pairwise t tests of original data values.

Reverse transcription-quantitative PCR analysis

RNA was extracted with Trizol and reverse transcribed with the SuperScript III First-Strand Synthesis System (Invitrogen). Quantitative PCR was performed as previously described (44). Primer sequences are listed in Supplementary Table S3.

Statistical analysis

The statistical analysis of data was based on Student's *t*-tests. Calculations were performed on a minimum of three independent data sets, assuming two-sample equal variance and a two-tailed distribution. Unless stated otherwise, significant difference is expressed using *t*-test at $p < 0.05$.

Acknowledgments

The authors thank the Salk Institute Genomic Analysis Laboratory for providing the sequence-indexed *Arabidopsis* T-DNA insertion mutants and the Nottingham Arabidopsis Stock Centre, UK, for the supply of seed stocks. They are grateful to Danielle Jaillard, Centre Commun de Microscopie Electronique, Université de Paris sud 11, France, for help with sample preparation for electron microscopy; to Jutta Hager, IBP, Orsay, France, for assistance during the initial production of the *cat2 cad2* mutant; and to Patrick Saindrenan (IBP) for providing HPLC facilities. This work was partly funded by the French Agence Nationale de la Recherche project "Vulnoz," the European Union Marie-Curie project "Chloroplast Signals," and the Austrian Science Fund (FWF P22988). G.Q. thanks the European Union for a Marie Curie individual fellowship grant (PIEF-GA-2009-252927: ROXNP). Y.H. was the recipient of a PhD grant from the Chinese Scholarship Council.

Author Disclosure Statement

No competing financial interests exist.

References

1. Apostol I, Heinstein PF, and Low PS. Rapid stimulation of an oxidative burst during elicitation of cultured plant cells: Role in defense and signal transduction. *Plant Physiol* 90: 109–116, 1989.
2. Baldacci-Cresp F, Chang C, Maucourt C, Deborde C, Hopkins J, Lecomte P, Bernillon S, Brouquisse R, Moing A, Abad P,

Hérouart D, Puppo A, Favery B, and Frendo P. (Homo)glutathione deficiency impairs root-knot nematode development in *Medicago truncatula*. *PLoS Pathog* 8: e1002471.
3. Ball L, Accotto G, Bechtold U, Creissen G, Funck D, Jimenez A, Kular B, Leyland N, Mejia-Carranza J, Reynolds H, Karpinski S, and Mullineaux PM. Evidence for a direct link between glutathione biosynthesis and stress defense gene expression in Arabidopsis. *Plant Cell* 16: 2448–2462, 2004.
4. Bashandy T, Guilleminot J, Vernoux T, Caparros-Ruiz D, Ljung K, Meyer Y, and Reichheld JP. Interplay between the NADP-linked thioredoxin and glutathione systems in Arabidopsis auxin signaling. *Plant Cell* 22: 376–391, 2010.
5. Bick JA, Setterdahl AT, Knaff DB, Chen Y, Pitcher LH, Zilinskas BA, and Leustek T. Regulation of the plant-type 5′-adenylyl sulfate reductase by oxidative stress. *Biochemistry* 40: 9040–9048, 2001.
6. Bindschedler LV, Dewdney J, Blee KA, Stone JM, Asai T, Plotnikov J, Denoux C, Hayes T, Gerrish C, Davies DR, Ausubel FM, and Bolwell GP. Peroxidase-dependent apoplastic oxidative burst in Arabidopsis required for pathogen resistance. *Plant J* 47: 851–863, 2006.
7. Cao H, Bowling SA, Gordon AS, and Dong X. Characterization of an Arabidopsis mutant that is nonresponsive to inducers of systemic acquired resistance. *Plant Cell* 6: 1583–1592, 1994.
8. Chaouch S and Noctor G. *Myo*-inositol abolishes salicylic acid-dependent cell death and pathogen defence responses triggered by peroxisomal H_2O_2. *New Phytol* 188: 711–718, 2010.
9. Chaouch S, Queval G, Vanderauwera S, Mhamdi A, Vandorpe M, Langlois-Meurinne M, Van Breusegem F, Saindrenan P, and Noctor G. Peroxisomal hydrogen peroxide is coupled to biotic defense responses by ISOCHORISMATE SYNTHASE 1 in a daylength-related manner. *Plant Physiol* 153: 1692–1705, 2010.
10. Chaouch S, Queval G, and Noctor G. AtRbohF is a crucial modulator of defence-associated metabolism and a key actor in the interplay between intracellular oxidative stress and pathogenesis responses in Arabidopsis. *Plant J* 69: 613–627, 2012.
11. Cobbett CS, May MJ, Howden R, and Rolls B. The glutathione-deficient, cadmium-sensitive mutant, *cad2-1*, of *Arabidopsis thaliana* is deficient in γ–glutamylcysteine synthetase. *Plant J* 16: 73–78, 1998.
12. Dat JF, Inzé D, and Van Breusegem F. Catalase-deficient tobacco plants: tools for in planta studies on the role of hydrogen peroxide. *Redox Rep* 6: 37–42, 2001.
13. Daudi A, Cheng Z, O'Brien JA, Mammarella N, Khan S, Ausubel FM, and Bolwell GP. The apoplastic oxidative burst peroxidase in Arabidopsis is a major component of pattern-triggered immunity. *Plant Cell* 24: 275–287, 2012.
14. Doke N. Involvement of superoxide anion generation in the hypersensitive response of potato tuber tissues to infection with an incompatible race of *Phytophthora infestans* and to the hyphal wall components. *Physiol Plant Pathol* 23: 345–357, 1983.
15. Donahue JL, Alford SR, Torabinejad J, Kerwin RE, Nourbakhsh A, Ray WK, Hernick M, Huang X, Lyons BM, Hein PP, and Gillaspy GE. The *Arabidopsis thaliana Myo*-inositol 1-phosphate synthase1 gene is required for *Myo*-inositol synthesis and suppression of cell death. *Plant Cell* 22: 888–903, 2010.
16. Dubreuil-Maurizi C, Vitecek J, Marty L, Branciard L, Frettinger P, Wendehenne D, Meyer AJ, Mauch F, and Poinssot B. Glutathione deficiency of the Arabidopsis mutant *pad2-1* affects oxidative stress-related events, defense gene expression, and the hypersensitive response. *Plant Physiol* 157: 2000–2012, 2011.
17. Edwards R, Blount JW, and Dixon RA. Glutathione and elicitation of the phytoalexin response in legume cell cultures. *Planta* 184: 403–409, 1991.
18. Foyer CH and Noctor G. Redox regulation in photosynthetic organisms: signaling, acclimation, and practical implications. *Antioxid Redox Signal* 11: 861–905, 2009.
19. Ghanta S, Bhattacharyya D, Sinha R, Banerjee A, and Chattopadhyay S. *Nicotiana tabacum* overexpressing γ-ECS exhibits biotic stress tolerance likely through NPR1-dependent salicylic acid-mediated pathway. *Planta* 233: 895–910, 2011.
20. Gomez LD, Noctor G, Knight MR, and Foyer CH. Regulation of calcium signalling and gene expression by glutathione. *J Exp Bot* 55: 1851–1859, 2004.
21. Gomez LD, Vanacker H, Buchner P, Noctor G, and Foyer CH. Intercellular distribution of glutathione synthesis and its response to chilling in maize. *Plant Physiol* 134: 1662–1671, 2004.
22. Gromes R, Hothorn M, Lenherr ED, Rybin V, Scheffzek K, and Rausch T. The redox switch of gamma-glutamylcysteine ligase via a reversible monomer-dimer transition is a mechanism unique to plants. *Plant J* 54: 1063–1075, 2008.
23. Hicks LM, Cahoon RE, Bonner ER, Rivard RS, Sheffield J, and Jez JM. Thiol-based regulation of redox-active glutamate-cysteine ligase from *Arabidopsis thaliana*. *Plant Cell* 19: 2653–2661, 2007.
24. Höller K, Király L, Künstler A, Müller M, Gullner G, Fattinger M, and Zechmann B. Enhanced glutathione metabolism is correlated with sulphur-induced resistance in Tobacco mosaic virus-infected genetically susceptible *Nicotiana tabacum* plants. *Mol Plant Microb Interact* 23: 1448–1459, 2010.
25. Király L, Künstler A, Höller K, Fattinger M, Juhász C, Müller M, Gullner G, and Zechmann B. Sulfate supply influences compartment specific glutathione metabolism and confers enhanced resistance to Tobacco mosaic virus during a hypersensitive response. *Plant Physiol Biochem* 59: 44–54, 2012.
26. Koornneef A, Leon-Reyes A, Ritsema T, Verhage A, Den Otter FC, Van Loon LC, and Pieterse CMJ. Kinetics of salicylate-mediated suppression of jasmonate signaling reveal a role for redox modulation. *Plant Physiol* 147: 1358–1368, 2008.
27. Laloi C, Mestres-Ortega D, Marco Y, Meyer Y, and Reichheld JP. The Arabidopsis cytosolic thioredoxin *h5* gene induction by oxidative stress and its W-box-mediated response to pathogen elicitor. *Plant Physiol* 134: 1006–1016, 2004.
28. Levine A, Tenhaken R, Dixon R, and Lamb C. H_2O_2 from the oxidative burst orchestrates the plant hypersensitive disease resistance response. *Cell* 79: 1–20, 1994.
29. Lindermayr C, Sell S, Müller B, Leister D, and Durner J. Redox regulation of the NPR1-TGA1 system of *Arabidopsis thaliana* by nitric oxide. *Plant Cell* 22: 2894–2907, 2010.
30. Liu G, Ji Y, Bhuiyan NH, Pilot G, Selvaraj G, Zou J, and Wei Y. Amino acid homeostasis modulates salicylic acid–associated redox status and defense responses in *arabidopsis*. *Plant Cell* 22: 3845–3863, 2010.
31. Marty L, Siala W, Schwarzländer M, Fricker MD, Wirtz M, Sweetlove LJ, Meyer Y, Reichheld JP, and Hell R. The NADPH-dependent thioredoxin system constitutes a functional backup for cytosolic glutathione reductase in *Arabidopsis*. *Proc Natl Acad Sci USA* 106: 9109–9114, 2009.

32. Mateo A, Funck D, Mühlenbock P, Kular B, Mullineaux PM, and Karpinski S. Controlled levels of salicylic acid are required for optimal photosynthesis and redox homeostasis. *J Exp Bot* 57: 1795–1807, 2006.
33. Maughan SC, Pasternak M, Cairns N, Kiddle G, Brach T, Jarvis R, Haas F, Nieuwland J, Lim B, Müller C, Salcedo-Sora E, Kruse C, Orsel M, Hell R, Miller AJ, Bray P, Foyer CH, Murray JA, Meyer AJ, and Cobbett CS. Plant homologs of the *Plasmodium falciparum* chloroquine-resistance transporter, *Pf*CRT, are required for glutathione homeostasis and stress responses. *Proc Natl Acad Sci USA* 107: 2331–2336, 2010.
34. May MJ, Parker JE, Daniels MJ, Leaver CJ, and Cobbett CS. An Arabidopsis mutant depleted in glutathione shows unaltered responses to fungal and bacterial pathogens. *Mol Plant Microb Int* 9: 349–356, 1996.
35. Meng PH, Raynaud C, Tcherkez G, Blanchet S, Massoud K, Domenichini S, Henry Y, Soubigou-Taconnat L, Lelarge-Trouverie C, Saindrenan P, Renou JP, and Bergounioux C. Crosstalks between *myo*-inositol metabolism, programmed cell death and basal immunity in *Arabidopsis*. *PLoS One* 4: e7364, 2009.
36. Mhamdi A, Hager J, Chaouch S, Queval G, Han Y, Taconnat L, Saindrenan P, Gouia H, Issakidis-Bourguet E, Renou JP, and Noctor G. *Arabidopsis* GLUTATHIONE REDUCTASE 1 plays a crucial role in leaf responses to intracellular H_2O_2 and in ensuring appropriate gene expression through both salicylic acid and jasmonic acid signaling pathways. *Plant Physiol* 153: 1144–1160, 2010.
37. Mhamdi A, Queval G, Chaouch S, Vanderauwera S, Van Breusegem F, and Noctor G. Catalase in plants: a focus on Arabidopsis mutants as stress-mimic models. *J Exp Bot* 61: 4197–4220, 2010.
38. Mou Z, Fan W, and Dong X. Inducers of plant systemic acquired resistance regulate NPR1 function through redox changes. *Cell* 113: 935–944, 2003.
39. Nikiforova V, Freitag J, Kempa S, Adamik M, Hesse H, and Hoefgen R. Transcriptome analysis of sulfur depletion in *Arabidopsis thaliana*: interlacing of biosynthetic pathways provides response specificity. *Plant J* 33: 633–650, 2003.
40. Noctor G. Metabolic signalling in defence and stress: the central roles of soluble redox couples. *Plant Cell Environ* 29: 409–425, 2006.
41. O'Brien JA, Daudi A, Finch P, Butt VS, Whitelegge JP, Souda P, Ausubel FM, and Bolwell GP. A peroxidase-dependent apoplastic oxidative burst in cultured arabidopsis cells functions in MAMP-elicited defense. *Plant Physiol* 158: 2013–2027, 2012.
42. Parisy V, Poinssot B, Owsianowski L, Buchala A, Glazebrook J. and Mauch F. Identification of PAD2 as a γ-glutamylcysteine synthetase highlights the importance of glutathione in disease resistance in Arabidopsis. *Plant J* 49: 159–172, 2007.
43. Queval G and Noctor G. A plate-reader method for the measurement of NAD, NADP, glutathione and ascorbate in tissue extracts. Application to redox profiling during *Arabidopsis* rosette development. *Anal Biochem* 363: 58–69, 2007.
44. Queval G, Issakidis-Bourguet E, Hoeberichts FA, Vandorpe M, Gakière B, Vanacker H, Miginiac-Maslow M, Van Breusegem F, and Noctor G. Conditional oxidative stress responses in the *Arabidopsis* photorespiratory mutant *cat2* demonstrate that redox state is a key modulator of daylength-dependent gene expression and define photoperiod as a crucial factor in the regulation of H_2O_2-induced cell death. *Plant J* 52: 640–657, 2007.
45. Queval G, Hager J, Gakière B, and Noctor G. Why are literature data for H_2O_2 contents so variable? A discussion of potential difficulties in quantitative assays of leaf extracts. *J Exp Bot* 59: 135–146, 2008.
46. Queval G, Thominet D, Vanacker H, Miginiac-Maslow M, Gakière B, and Noctor G. H_2O_2-activated up-regulation of glutathione in Arabidopsis involves induction of genes encoding enzymes involved in cysteine synthesis in the chloroplast. *Mol Plant* 2: 344–356, 2009.
47. Queval G, Jaillard D, Zechmann B, and Noctor G. Increased intracellular H_2O_2 availability preferentially drives glutathione accumulation in vacuoles and chloroplasts. *Plant Cell Environ* 34: 21–32, 2011.
48. Rate DN, Cuenca JV, Bowman DS, and Greenberg JT. The gain-of-function Arabidopsis *acd6* mutant reveals novel regulation and function of the salicylic acid signaling pathway in controlling cell death, defenses, and cell growth. *Plant Cell* 11: 1695–1708, 1999.
49. Reichheld JP, Khafif M, Riondet C, Bonnard G, and Meyer Y. Inactivation of thioredoxin reductases reveals a complex interplay between thioredoxin and glutathione pathways in Arabidopsis development. *Plant Cell* 19: 1851–1865, 2007.
50. Rizhsky L, Hallak-Herr E, Van Breusegem F, Rachmilevitch S, Barr JE, Rodermel S, Inzé D, and Mittler R. Double antisense plants lacking ascorbate peroxidase and catalase are less sensitive to oxidative stress than single antisense plants lacking ascorbate peroxidase or catalase. *Plant J* 32: 329–342, 2002.
51. Rojas CM, Senthil-Kumar M, Wang K, Ryu CM, Kaundal A, and Mysore KS. Glycolate oxidase modulates reactive oxygen species-mediated signal transduction during nonhost resistance in *Nicotiana benthamiana* and *Arabidopsis*. *Plant Cell* 24: 336–352, 2012.
52. Schlaeppi K, Bodenhausen N, Buchala A, Mauch F, and Reymond P. The glutathione-deficient mutant *pad2-1* accumulates lower amounts of glucosinolates and is more susceptible to the insect herbivore *Spodoptera littoralis*. *Plant J* 55: 774–786, 2008.
53. Sen Gupta A, Alscher RG, and McCune D. Response of photosynthesis and cellular antioxidants to ozone in *Populus* leaves. *Plant Physiol* 96: 650–655, 1991.
54. Shah J, Kachroo P, Nandi A, and Klessig DF. A recessive mutation in the *Arabidopsis SSI2* gene confers SA- and *NPR1*-independent expression of *PR* genes and resistance against bacterial and oomycete pathogens. *Plant J* 25: 563–574, 2001.
55. Shirano Y, Kachroo P, Shah J, and Klessig DF. A gain-of-function mutation in an Arabidopsis Toll Interleukin1 Receptor–Nucleotide Binding Site–Leucine-Rich Repeat type R gene triggers defense responses and results in enhanced disease resistance. *Plant Cell* 14: 3149–3162, 2002.
56. Smith IK, Kendall AC, Keys AJ, Turner JC, and Lea PJ. Increased levels of glutathione in a catalase-deficient mutant of barley (*Hordeum vulgare* L.). *Plant Sci Lett* 37: 29–33, 1984.
57. Spoel SH, Koornneef A, Claessens SM, Korzelius JP, Van Pelt JA, Mueller MJ, Buchala AJ, Métraux JP, Brown R, Kazan K, Van Loon LC, Dong X, and Pieterse CM. NPR1 modulates cross-talk between salicylate- and jasmonate-dependent defense pathways through a novel function in the cytosol. *Plant Cell* 15: 760–770, 2003.
58. Strawn MA, Marr SK, Inoue K, Inada N, Zubieta C, and Wildermuth MC. *Arabidopsis* isochorismate synthase functional in pathogen-induced salicylate biosynthesis exhibits properties consistent with a role in diverse stress responses. *J Biol Chem* 282: 5919–5933, 2007.

59. Tada Y, Spoel SH, Pajerowska-Mukhtar K, Mou Z, Song J, Wang C, Zuo J, and Dong X. Plant immunity requires conformational charges of NPR1 via S-nitrosylation and thioredoxins. *Science* 321: 952–956, 2008.
60. Torres MA, Dangl JL, and Jones JD. *Arabidopsis* $gp91^{phox}$ homologues *AtrbohD* and *AtrbohF* are required for accumulation of reactive oxygen intermediates in the plant defense response. *Proc Natl Acad Sci USA* 99: 517–522, 2002.
61. Torres MA, Jones JD, and Dangl JL. Pathogen-induced, NADPH oxidase–derived reactive oxygen intermediates suppress spread of cell death in *Arabidopsis thaliana*. *Nat Genet* 37: 1130–1134, 2005.
62. Vanacker H, Carver TL, and Foyer CH. Early H_2O_2 accumulation in mesophyll cells leads to induction of glutathione during the hyper-sensitive response in the barley-powdery mildew interaction. *Plant Physiol* 123: 1289–1300, 2000.
63. Vanderauwera S, Suzuki N, Miller G, van de Cotte B, Morsa S, Ravanat JL, Hegie A, Triantaphylidès C, Shulaev V, Van Montagu MC, Van Breusegem F, and Mittler R. Extranuclear protection of chromosomal DNA from oxidative stress. *Proc Natl Acad Sci USA* 108: 1711–1716, 2011.
64. Vlot AC, Dempsey DA. and Klessig DF. Salicylic acid, a multifaceted hormone to combat disease. *Annu Rev Phytopathol* 47: 177–206, 2009.
65. Wachter A, Wolf S, Steininger H, Bogs J, and Rausch T. Differential targeting of GSH1 and GSH2 is achieved by multiple transcription initiation: implications for the compartmentation of glutathione biosynthesis in the *Brassicaceae*. *Plant J* 41: 15–30, 2005.
66. Wildermuth MC, Dewdney J, Wu G, and Ausubel FM. Isochorismate synthase is required to synthesize salicylic acid for plant defence. *Nature* 414: 562–565, 2001.
67. Willekens H, Chamnongpol S, Davey M, Schraudner M, Langebartels C, Van Montagu M, Inzé D, and Van Camp W. Catalase is a sink for H2O2 and is indispensable for stress defense in C3 plants. *EMBO J* 16: 4806–4816, 1997.
68. Winter H, Robinson DG, and Heldt HW. Subcellular volumes and metabolite concentrations in spinach leaves. *Planta* 193: 530–535, 1994.
69. Zechmann B and Müller M. Subcellular compartmentation of glutathione in dicotyledonous plants. *Protoplasma* 246: 15–24, 2010.
70. Zechmann B, Zellnig G, Urbanek-Krajnc A, and Müller M. Artifical elevation of glutathione affects symptom development in ZYMV-infected *Cucurbita pepo* L. plants. *Arch Virol* 152: 747–762, 2007.
71. Zhang Y, Goritschnig S, Dong X, and Li X. A gain-of-function mutation in a plant disease resistance gene leads to constitutive activation of downstream signal transduction pathways in *suppressor of npr1-1*, *constitutive 1*. *Plant Cell* 15: 2636–2646, 2003.

Address correspondence to:
Prof. Graham Noctor
Institut de Biologie des Plantes
UMR CNRS 8618
Université de Paris sud 11
Orsay Cedex 91405
France

E-mail: graham.noctor@u-psud.fr

Date of first submission to ARS Central, October 30, 2012; date of acceptance, November 11, 2012.

Abbreviations Used

CAT = catalase
γ-ECS = γ-glutamylcysteine synthetase
GC-TOF-MS = gas chromatography-time of flight-mass spectrometry
GR1 = glutathione reductase 1
GSH = reduced glutathione
GSSG = glutathione disulfide
hpi = hours post inoculation
ICS1 = isochorismate synthase
NPR1 = nonexpressor of pathogenesis-related 1
PR1 = pathogenesis-related 1
ROS = reactive oxygen species
SA = salicylic acid